Stable Negative Optical Torque in Optically Bound Nanoparticle Dimers

Tailei Qi, Fei Han, Wenbo Liu, and Zijie Yan*

Department of Applied Physical Sciences, University of North Carolina at Chapel Hill, Chapel Hill, NC 27599, United States

Abstract: Negative optical torque is a counterintuitive optomechanical phenomenon that can emerge in light-assembled nanoparticle (NP) clusters (*i.e.*, optical matter) under circular polarization. However in experiments, stable negative torque was limited to optical matter with 3 or more NPs. Here we show that by increasing the particle size, the sign of optical torque can be reversed in optical matter dimers, where stable negative torque arises in dimers of 300 nm diameter Au or 490 nm diameter polystyrene NPs. Our computational analysis reveals that the multipolar resonances in large NPs can enhance the forward scattering along the spin angular momentum (SAM) direction of light, creating a recoil negative torque due to momentum conservation. The observation of stable negative torque in dimers pushes the limit to the smallest optical matter, demonstrating the universal existence of negative torque in such a system. The underlying principle also provides new strategies for making light-driven nanomotors.

TOC

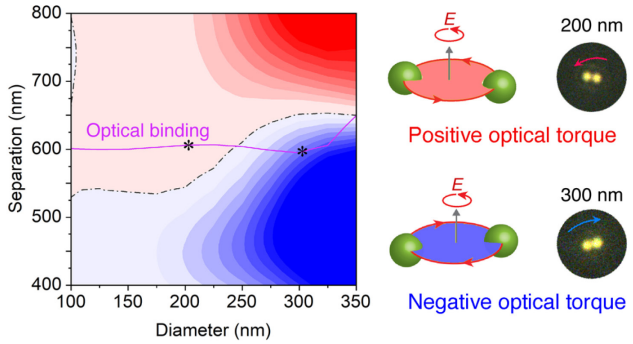

Keywords: Negative optical torque, optical binding, self-assembly, nanoparticle, light-matter interaction

Light carries momentum that can be transferred to small objects to induce observable motion. Sometimes the motion is counterintuitive. For example, the transfer of linear momentum from photons to an object normally generates a positive optical force to push the object forward. However, negative (or pulling) optical forces have also been predicted and observed under specific light-matter interactions.[1-5] Similarly, the transfer of SAM from circularly polarized light to an object normally creates positive optical torque to rotate the object along the SAM direction. However, under certain circumstances negative optical torque may also appear.[6-17] Negative optical torque was first observed in birefringent nanostructured glass slabs,[7] and later in macro-structured liquid-crystal polymer layers by the same research group.[15] In both studies, the generation of negative optical torque relies on inhomogeneous materials with structured birefringence. In contrast, a theoretical study predicted that even non-birefringent particles, *e.g.*, dielectric polystyrene microparticles, may also generate negative optical torque when they are arranged into discrete arrays with suitable interparticle separations.[8] This prediction has been demonstrated in light-assembled NP arrays,[14, 17, 18] where optical binding[19, 20] in a circularly polarized laser beam organized colloidal metal NPs into hexagonal clusters. The theoretical study argued that small clusters do not favor negative optical torque.[8] Our calculation also showed that under the point dipole approximation and only first-order scattering, the optical torque is always positive on a dimer and a trimer with linear configuration, while a trimer with trianglar configuration will show negative torque.[14] In our previous experiments, negative torque was only observed in optical matter with 3 or more NPs.[14, 17, 18] This result agrees with another experimental study, where negative optical torque appeared transiently when two Ag NPs fluctuated into a near-field separation, yet at the optical binding separation (close to λ_m - the wavelength of light in the medium around the NPs), only positive optical torque existed.[13]

A question arises whether stable negative optical torque can be created in two optically bound NPs. A hint was given by a theoretical study[6] published much earlier than other seminal work on negative (or left-handed) optical torque.[7, 8] In this study, the calculated positive optical torque in an optical matter dimer reversed the sign at certain particle sizes beyond the Rayleigh regime, *e.g.*, for silica particles with diameters of ~$0.5\lambda_m$.[6] This suggests that stable negative optical torque may be created in optical matter dimers with large NPs. In contrast, nearly all previous experiments used metal NPs with diameters around 0.19-$0.38\lambda_m$.[13, 14, 17, 18] It is worth checking whether optical binding of larger NPs will lead to different dynamics under circular polarization.

Here we report negative optical torque in optically bound Au NP dimers with diameters of 300 nm (corresponding to $0.5\lambda_m$ of the trapping laser) in a circularly polarized optical trap. We clearly show the reversal of optical torque from positive to negative when the particle size gradually increases from 100 nm to 300 nm with an interval of 50 nm. Our calculations reveal that the multipolar resonances become significant for Au NPs larger than 250 nm, which enhance the forward scattering along the SAM direction of light and create a recoil torque, *i.e.*, the negative optical torque. The phenomenon was also observed in optical matter dimers of polystyrene NPs with diameters of 490 nm. These results push the limit of negative optical torque to the smallest optical matter, demonstrating the universal existence of negative torque in the optical matter system.

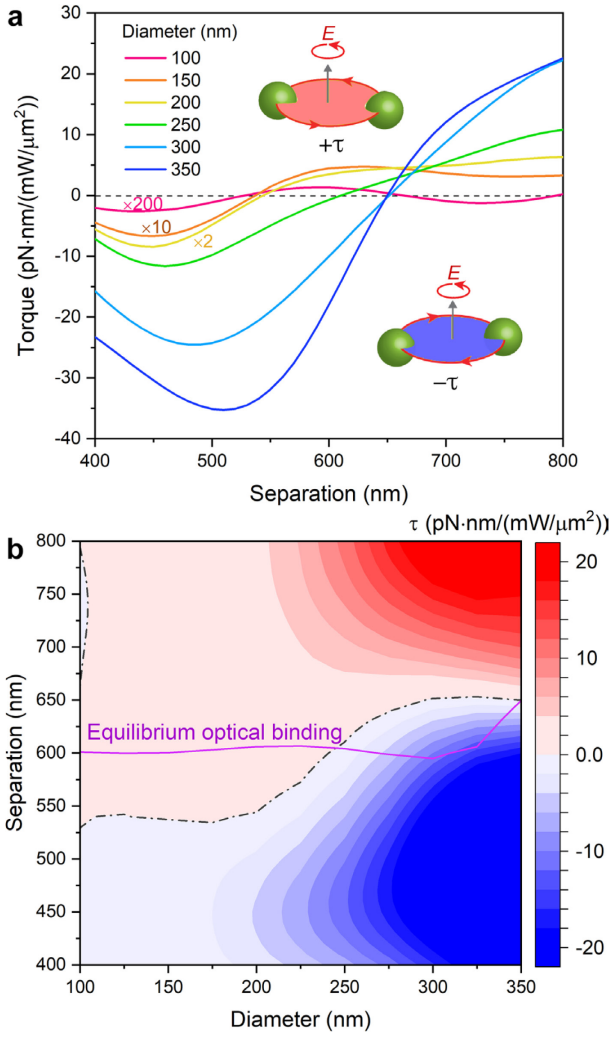

Figure 1. Calculated optical torque on dimers of Au NPs. (a) Optical torque on dimers with different particle sizes and interparticle separations. The torque curves for three small sizes are magnified by 2 to

200 times for better visualization. The insets illustrate the rotation directions of the electric vector of light and the dimer in the cases of positive and negative torques, respectively. (b) An optical torque diagram for dimers of Au NPs. The dashed black curves are the transition boundaries between positive and negative torques. The solid purple curve represents the interparticle separation of NPs at their equilibrium optical binding conditions.

In order to obtain stable optical torque in optically bound NP dimers, we chose plamonic Au NPs due to their ultrastrong optical binding and the commercial availability of different particle sizes in the submicron range.[17, 21, 22] To guide the selection of suitable particle sizes for experiments, we first calculated the optical torque on dimers of different particle sizes and interparticle separations using finite-difference time-domain (FDTD) simulations (see Supporting Information, Methods). In the simulations, the Au NPs (spheres) were confined in the *x*-*y* plane and illuminated by a circularly polarized laser in water (λ_m = 600 nm). The laser wave vector was in the *z*-direction and the electric vector *E* rotates counterclockwise (*i.e.*, the SAM direction). The results are shown in Fig. 1a and further interpolated into an optical torque diagram in Fig. 1b (see Fig. S1 in Supporting Information for additional data). Negative optical torque generally exists for small interparticle separations at a certain particle size, and positive torque exists for large separations. In particular, the optical torque diagram predicts an optical torque reversal in optical matter dimers with increasing NP sizes. When dimers are at their equilibrium optical binding separations, those with particle sizes less than 250 nm will generate positive optical torque, which is consistent with previous computational and experimental reports on NP dimers based on dipole approximations.[13, 14, 17, 18] However, when the particle sizes are between 250 nm and 350 nm, their corresponding dimers will experience negative optical torque at their optical binding separation. It is worth noting that Au dimers with smaller NPs can also experience negative optical torque at nonequilibrium separations,[13] *e.g.*, a dimer of 150 nm diameter NPs at 450 nm separation, but the torque is not stable since the dimer cannot maintain this separation by optical binding.

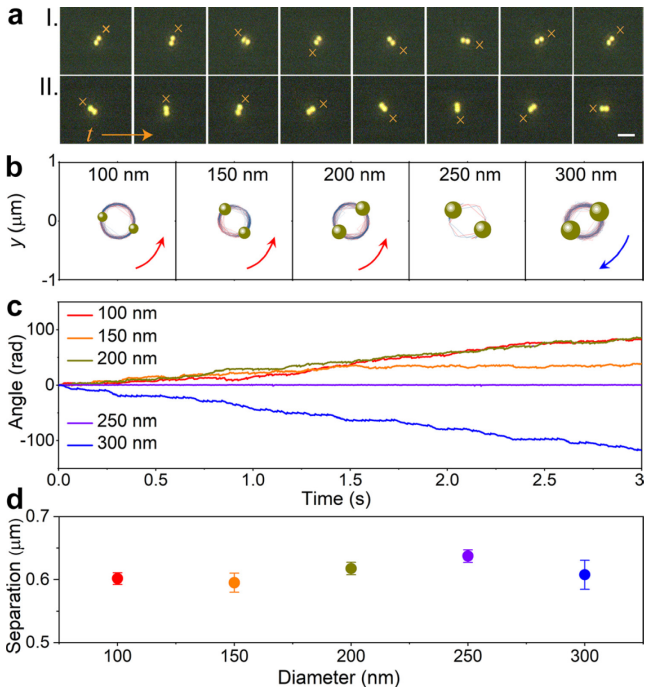

Figure 2. Optical torque reversal in optical matter dimers with increasing particle sizes. (a) Continuous frames of dark-field optical images of I. 200 nm and II. 300 nm diameter Au NP dimers rotating in the opposite directions in a circularly polarized optical trap. The *E* vector of light rotates counterclockwise in the imaging plane. The cross markers are used to track the rotation directions. The scale bar is 1 μm. (b) Trajectories of five dimers with different NP diameters relative to the center of mass of each dimer. Arrows indicate the rotation directions of the dimers. (c) The corresponding angular trajectory of the orientation of each dimer. (d) The interparticle separation of each dimer.

Guided by the simulation results, we conducted optical binding experiments with a series of Au NPs in the size range of 100-300 nm (see Supporting Information, Fig. S2). The NPs were trapped near a coverslip surface in water by a collimated laser beam (λ_m = 600 nm) with circular polarization and relatively flat intensity (see Supporting Information, Methods). The traditional optical trap, *i.e.*, a tightly focused Gaussian beam, is not suitable for the experiments because the strong compressive gradient force could easily collapse the optical binding configuration.[23] The optically bound NP dimers normally rotate around their centers of mass, but the directon can change for different particle sizes, which can be clearly seen from the dark-field optical images in Fig. 2a and the trajectories of NPs plotted in Fig. 2b (also see Supporting Information, Video S1). Figure 2c further shows the unwrapped angular trajectories of the two NPs relative to their centers of mass. The rotational direction of a dimer clearly depends on the size of the constituent NPs. The

dimers of 100, 150 and 200 nm Au NPs have positive angular velocities (*i.e.*, the slopes of trajectories), but the dimer with 300 Au NPs has a negative angular velocity, while the dimer with 250 nm Au NPs just fluctuates without directional rotation. Figure 2d shows the interparticle separations of these dimers, which are very close to the calculated optical binding separations (see Fig. S3 in Supporting Information). Since the *E* vector of light rotates counterclockwise, positive angular velocity corresponds to positive optical torque. Therefore, the results confirm the size-dependent optical torque reversal from positive to negative in the Au NP dimers, where the crossover occurs around 250 nm diameter. We have examined the rotation directions of multiple dimers for each NP size and confirmed that 100-200 nm NP dimers have positive torque while 300 nm NP dimers have negative torque (Fig. S4 in Supporting Information). These experimental results agree very well with the simulation predictions.

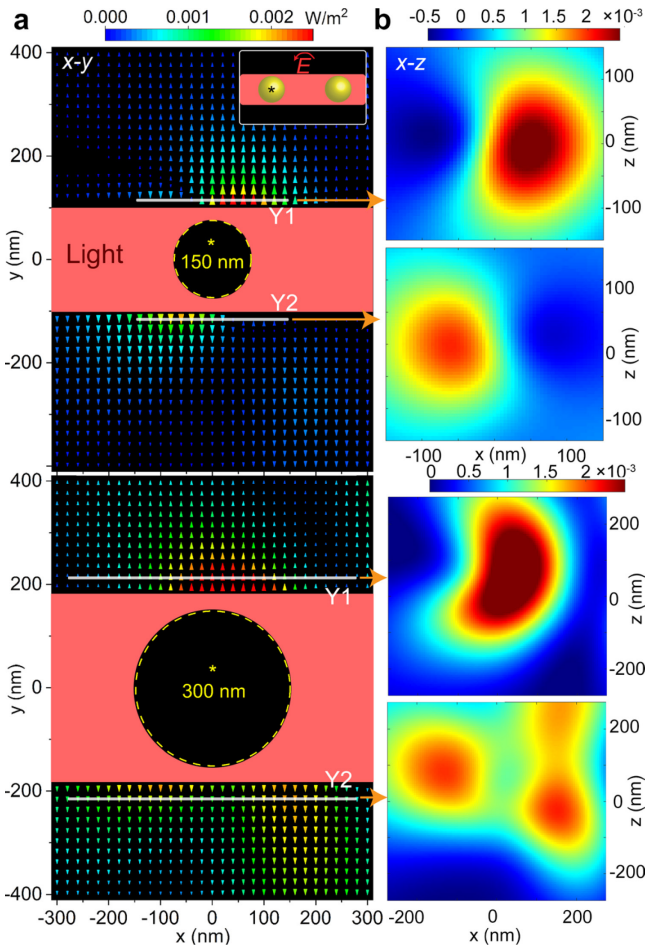

Figure 3. Calculated light scattering by a 150 nm and a 300 nm Au NP in their corresponding dimer system. (a) The *y*-components of Poynting vectors around the two NPs in the *x*-*y* plane. The directions are shown

by the arrows and the magnitudes are mapped by the colors. Each NP is left in a dimer oriented along the *x*-axis as illustrated in the top-right inset of the top panel. The interparticle separation is 600 nm. The red strip indicates the area illuminated by circularly polarized light (λ_m = 600 nm). Y1 and Y2 are two monitors placed in the *x*-*z* plane to record the light scattering by each NP in the +*y* and –*y* directions. (b) The *y*-components of Poynting vectors across the Y1 and Y2 monitors. Positive values on the Y1 and Y2 monitors indicate that the light power flows in the +*y* and –*y* directions, respectively.

Negative optical torque also occurs in polystyrene NP dimers. We have trapped polystyrene dimers of 170 nm, 260 nm, 300 nm, and 490 nm (see Supporting Information, Fig. S5). Stable negative optical torque was observed in polystyrene dimers of a 490 nm diameter (see Supporting Information, Fig. S6 and Video S2) as predicted by simulations (see Supporting Information, Fig. S7).

To understand the size-dependent reversal of optical torque, we calculated the Poynting vectors around the NPs in their dimers and monitor the light scattering. As illustrated in the top-right inset of Fig. 3a, the FDTD simulation model places two NPs along the *x*-axis, so the difference of light scattering in the +*y* and –*y* directions by each NP can indicate the optical force and torque on this NP. The two NPs are illuminated by a narrow strip of light (projection of a 3-dimensional light source in the *x*-*y* plane) that propagates in the +*z* direction, and two monitors (Y1 and Y2) are placed in the *x*-*z* plane close to the left NP to record the scattering power of light. Figure 3a shows the *y*-components of Poynting vectors of scattered light on the *x*-*y* plane at $z = 0$ across the centers of a 150 nm and a 300 nm Au NP in two dimers (see Supporting Information, Fig. S8 for Poynting vectors with both *x* and *y*-components). Both NPs have a strong scattering region away from the NP surface in the +*y* direction, which can be seen from the red region of the Poynting vectors. Similar scattering behavior can be observed in the Y1 monitors as shown in Fig. 3b. However, the scattering in the –*y* direction shows different behaviors for the two NPs, while the 150 nm NP has one scattering region to its bottom-left side on the *x*-*z* plane, the 300 nm NP has another elongated scattering region to its bottom-right side. This additional scattering region is due to the multipolar resonances in the large Au NPs. By calculating the multipolar expansion of the scattering cross-sections of Au NPs, we find that the total scattering of a Au NP is almost solely contributed by the electric dipole when the particle diameter $d \leq 200$ nm, while for larger particles the magnetic dipole and electric quadrupole start to arise (Supporting Information, Fig. S9). For dimers, the electric quadrupole starts to arise in smaller NPs at 150 nm. Therefore, the

dipole approximation is suitable for describing the optical binding of Au NP dimers up to 150 nm diameter, corresponding to $0.25\lambda_m$, but not accurate anymore for larger particles.

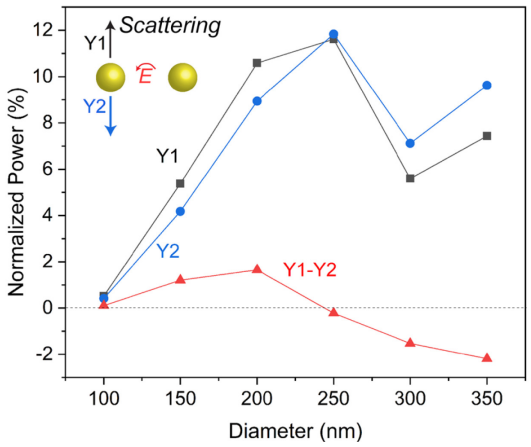

Figure 4. Light scattering in the +*y* (Y1) and –*y* (Y2) directions by the left NPs of different sizes in their corresponding dimers. The power of scattered light is normalized to the power of incident light. Y1–Y2 is the net power of the scattering, where the negative value indicates enhanced scattering along the SAM direction of light.

It is known that negative optical torque can arise in a discrete particle assembly when its scattering increases the SAM of light along the positive direction.[8, 9] Therefore, the additional scattering region in Fig. 3b may enhance the scattering to the –*y* direction and cause a different optical torque on the 300 nm NP. To verify that, we further checked the power of scattered light across the Y1 and Y2 planes for the 150 nm and 300 nm NPs. As shown in Fig. 4, the two NPs indeed have different biases of scattering, where the 150 nm NP scatters more strongly in the +*y* direction while the 300 nm NP scatters more strongly in the –*y* direction. Similar bias is observed in the projection of the angular intensity distribution of scattering from 300 nm Au NP dimers (Supporting Information, Fig. S10). Additional NP sizes have also been examined, and a trend of reversed net scattering, as represented by the difference of scattering power (P) across the two monitors (*i.e.*, P_{Y1}–P_{Y2}), can be clearly seen in Fig. 4. In particular, the net negative scattering power for NPs larger than 250 nm indicates stronger scattering in the –*y* direction, which will generate a recoil force to move the NPs along the +*y* direction. As a result, the dimer will rotate clockwise, which is opposite to the rotation direction of the *E* vector of light and is driven by a negative optical torque. In other words, the enhanced scattering along the SAM direction by a

dimer of larger NPs increases the angular momentum of light, and due to the momentum conservation in the system (*i.e.*, the dimer and light), the dimer needs to rotate in the opposite direction, leading to a negative torque. This mechanism can also be applied to explain the optical torque reversal *via* changing the interparticle separation of a dimer. For example, Fig. 1 predicts that for a dimer of 300 Au NPs, the optical torque will reverse from negative back to positive by increasing the interparticle separation from 600 nm to 700 nm. Our calculations confirm that the net scattering power flow indeed evolves from the $-y$ to $+y$ direction with the crossover at 650 nm (see Supporting Information, Fig. S11), the same as that in Fig. 1.

Since the optical trapping beam only carries SAM, the orbital motions of the dimers must come from the spin-to-orbital angular momentum conversion.[6] Such conversion can be induced even by a single sphere, which is manifested by a spiral energy flow (*i.e.*, the Poynting vector) of the scattering field around the sphere.[24] Our simulations show that such spiral energy flows exist around single Au NPs (see Supporting Information, Fig. S12). Moreover, we find that for a 150 nm Au NP, the energy flow will only exert a positive optical torque on a virtual 150 nm Au NP (without interparticle interactions) at the optical binding position, while for a 300 nm Au NP, two opposite energy flows exist one of which will generate a negative optical torque. In real optical matter dimers, the interparticle interactions are dominant as shown in Figs. 3 and 4, but the single particle cases still indicate that the particle size can influence the sign of optical torque by changing the spin-to-orbital angular momentum conversion.

In conclusion, we have demonstrated that stable negative optical torque can exist in the simplest optical matter clusters, *i.e.*, a dimer. This result reduces the required number of constituent particles to observe this phenomenon in the optical matter system from at least 3 down to 2, which could not be achieved in previous studies despite various efforts such as tuning the surface charge and laser wavelength.[13, 14, 17, 18] The solution relies on the particle size, where multipolar resonances arise in large NPs that enhance the forward scattering along the SAM direction of light, leading to negative optical torque due to the conservation of momentum. We have used both Au and polystyrene NPs to experimentally show this phenomenon, which demonstrates the universal existence of negative torque in the optical matter system. We have also used FDTD simulations and numerical calculations to reveal the mechanism, which provides a clear understanding of the seemingly abnormal dynamics of NPs in an optical field. NP dimers are of general interests for their potential applications in nanomotors and nanoswimmers,[25-28] *e.g.*, lateral optical forces can

arise in asymmetric NP dimers with different particle sizes,[25, 29] and recently this principle has been applied to fabricate nanomotors and metavehicles based on arrays of asymmetric NP dimers.[30, 31] One may view the negative optical torque in optical matter as a special product of lateral optical force, considering that the force is also orthogonal to the beam propagation direction and arises from non-conservative electrodyanmic interactions.[6] Controlling and switching the sign of optical torque on metasurfaces based on discrete NP clusters by changing the particle size, along with other parameters such interparticle separation, number and configuration of constituent NPs, will provide new strategies to fabricate and manipulate nanomotors.

ASSOCIATED CONTENT

Supporting Information

The Supporting Information is available free of charge on the ACS Publications website at

Methods, additional figures and notes (PDF)

Motions of Au NP dimers with different diameters from 100 nm to 300 nm (the frame rate is slowed down by 6 times for better viewing) (AVI)

Motions of polystyrene NP dimers with different diameters from 170 nm to 490 nm (the frame rate is slowed down by 2 times for better viewing) (AVI)

AUTHOR INFORMATION

Corresponding Author

Zijie Yan − *Department of Applied Physical Sciences, University of North Carolina at Chapel Hill, Chapel Hill, NC 27599, United States;* orcid.org/0000-0003-0726-7042

E-mail: zijieyan@unc.edu

Authors

Tailei Qi − *Department of Applied Physical Sciences, University of North Carolina at Chapel Hill, Chapel Hill, NC 27599, United States*

Fei Han − *Department of Applied Physical Sciences, University of North Carolina at Chapel Hill, Chapel Hill, NC 27599, United States*

Wenbo Liu − *Department of Applied Physical Sciences, University of North Carolina at Chapel Hill, Chapel Hill, NC 27599, United States*

Author Contributions

Z.Y. conceived the project. T.Q., F.H. and W.L. carried out the experiments. T.Q. and F.H. analyzed the data. Z.Y. performed the calculations and simulations. T.Q. and Z.Y. wrote the manuscript.

Notes

The authors declare no competing financial interest.

ACKNOWLEDGMENTS

This material is based upon work supported by the National Science Foundation under Grant No. 2131079. The authors thank Norbert F. Scherer and John A. Parker for helpful discussions on the multipole analysis and experimental results.

REFERENCES

1. Novitsky, A.; Qiu, C. W.; Wang, H., Single gradientless light beam drags particles as tractor beams. *Phys. Rev. Lett.* **2011,** *107*, 203601.
2. Sukhov, S.; Dogariu, A., Negative nonconservative forces: optical "tractor beams" for arbitrary objects. *Phys. Rev. Lett.* **2011,** *107*, 203602.
3. Chen, J.; Ng, J.; Lin, Z.; Chan, C. T., Optical pulling force. *Nat. Photon.* **2011,** *5*, 531-534.
4. Brzobohatý, O.; Karásek, V.; Šiler, M.; Chvátal, L.; Čižmár, T.; Zemánek, P., Experimental demonstration of optical transport, sorting and self-arrangement using a 'tractor beam'. *Nat. Photon.* **2013,** *7*, 123-127.
5. Shvedov, V.; Davoyan, A. R.; Hnatovsky, C.; Engheta, N.; Krolikowski, W., A long-range polarization-controlled optical tractor beam. *Nat. Photon.* **2014,** *8*, 846-850.
6. Haefner, D.; Sukhov, S.; Dogariu, A., Conservative and nonconservative torques in optical binding. *Phys. Rev. Lett.* **2009,** *103*, 173602.
7. Hakobyan, D.; Brasselet, E., Left-handed optical radiation torque. *Nat. Photon.* **2014,** *8*, 610-614.
8. Chen, J.; Ng, J.; Ding, K.; Fung, K. H.; Lin, Z.; Chan, C. T., Negative optical torque. *Sci. Rep.* **2014,** *4*, 6386.
9. Nieto-Vesperinas, M., Optical torque on small bi-isotropic particles. *Opt. Lett.* **2015,** *40*, 3021-3024.
10. Hakobyan, D.; Brasselet, E., Optical torque reversal and spin-orbit rotational Doppler shift experiments. *Opt. Express* **2015,** *23*, 31230-31239.
11. Canaguier-Durand, A.; Genet, C., Chiral route to pulling optical forces and left-handed optical torques. *Phys. Rev. A* **2015,** *92*, 043823.
12. Mitri, F. G., Negative optical spin torque wrench of a non-diffracting non-paraxial fractional Bessel vortex beam. *J. Quant. Spectrosc. Radiat. Transf.* **2016,** *182*, 172-179.
13. Sule, N.; Yifat, Y.; Gray, S. K.; Scherer, N. F., Rotation and Negative Torque in Electrodynamically Bound Nanoparticle Dimers. *Nano Lett.* **2017,** *17*, 6548-6556.

14. Han, F.; Parker, J. A.; Yifat, Y.; Peterson, C.; Gray, S. K.; Scherer, N. F.; Yan, Z., Crossover from positive to negative optical torque in mesoscale optical matter. *Nat. Commun.* **2018,** *9*, 4897.
15. Magallanes, H.; Brasselet, E., Macroscopic direct observation of optical spin-dependent lateral forces and left-handed torques. *Nat. Photon.* **2018,** *12*, 461-464.
16. Diniz, K.; Dutra, R. S.; Pires, L. B.; Viana, N. B.; Nussenzveig, H. M.; Maia Neto, P. A., Negative optical torque on a microsphere in optical tweezers. *Opt. Express* **2019,** *27*, 5905-5917.
17. Han, F.; Yan, Z., Phase transition and self-stabilization of light-mediated metal nanoparticle assemblies. *ACS Nano* **2020,** *14*, 6616-6625.
18. Parker, J.; Peterson, C. W.; Yifat, Y.; Rice, S. A.; Yan, Z.; Gray, S. K.; Scherer, N. F., Optical matter machines: angular momentum conversion by collective modes in optically bound nanoparticle arrays. *Optica* **2020,** *7*, 1341-1348.
19. Burns, M. M.; Fournier, J. M.; Golovchenko, J. A., Optical binding. *Phys. Rev. Lett.* **1989,** *63*, 1233-1236.
20. Dholakia, K.; Zemánek, P., Colloquium: Gripped by light: Optical binding. *Rev. Mod. Phys.* **2010,** *82*, 1767-1791.
21. Demergis, V.; Florin, E. L., Ultrastrong optical binding of metallic nanoparticles. *Nano Lett.* **2012,** *12*, 5756-60.
22. Nan, F.; Yan, Z., Sorting metal nanoparticles with dynamic and tunable optical driven forces. *Nano Lett.* **2018,** *18*, 4500-4505.
23. Yan, Z.; Gray, S. K.; Scherer, N. F., Potential energy surfaces and reaction pathways for light-mediated self-organization of metal nanoparticle clusters. *Nat. Commun.* **2014,** *5*, 3751.
24. Haefner, D.; Sukhov, S.; Dogariu, A., Spin Hall effect of light in spherical geometry. *Phys. Rev. Lett.* **2009,** *102*, 123903.
25. Yifat, Y.; Coursault, D.; Peterson, C. W.; Parker, J.; Bao, Y.; Gray, S. K.; Rice, S. A.; Scherer, N. F., Reactive optical matter: light-induced motility in electrodynamically asymmetric nanoscale scatterers. *Light Sci. Appl.* **2018,** *7*, 105.
26. Pile, D. F. P., Dimer nanomotors. *Nat. Photon.* **2019,** *13*, 139-139.
27. Klotsa, D., As above, so below, and also in between: mesoscale active matter in fluids. *Soft Matter* **2019,** *15*, 8946-8950.
28. Dombrowski, T.; Klotsa, D., Kinematics of a simple reciprocal model swimmer at intermediate Reynolds numbers. *Phys. Rev. Fluids* **2020,** *5*, 063103.
29. Sukhov, S.; Shalin, A.; Haefner, D.; Dogariu, A., Actio et reactio in optical binding. *Opt. Express* **2015,** *23*, 247-52.
30. Andren, D.; Baranov, D. G.; Jones, S.; Volpe, G.; Verre, R.; Kall, M., Microscopic metavehicles powered and steered by embedded optical metasurfaces. *Nat. Nanotechnol.* **2021,** *16*, 970-974.
31. Tanaka, Y. Y.; Albella, P.; Rahmani, M.; Giannini, V.; Maier, S. A.; Shimura, T., Plasmonic linear nanomotor using lateral optical forces. *Sci. Adv.* **2020,** *6*, eabc3726.